BRNO UNIVERSITY OF TECHNOLOGY
VYSOKÉ UČENÍ TECHNICKÉ V BRNĚ

FACULTY OF ELECTRICAL ENGINEERING AND COMMUNICATION
FAKULTA ELEKTROTECHNIKY
A KOMUNIKAČNÍCH TECHNOLOGIÍ

DEPARTMENT OF PHYSICS
ÚSTAV FYZIKY

CHARGE TRANSPORT AND STORAGE IN A SUPERCAPACITOR STRUCTURE
TRANSPORT A UKLÁDÁNÍ NÁBOJE VE STRUKTUŘE SUPERKONDENZÁTORU

DOCTORAL THESIS – SHORT VERSION
DIZERTAČNÍ PRÁCE – TEZE

AUTHOR
AUTOR PRÁCE
Ing. Tomáš Kuparowitz

SUPERVISOR
ŠKOLITEL
doc. Ing. Petr Sedlák, Ph.D.

BRNO 2017

Keywords

Supercapacitor, ultracapacitor, double-layer capacitor, supercapacitor equivalent circuit model, electrical charge redistribution in supercapacitor, supercapacitor parameters degradation.

Klíčová slova

Superkondenzátor, náhradní elektrický obvod superkondenzátoru, přerozdělení elektrického náboje v superkondenzátoru, degradace parametrů superkondenzátoru.

Place of thesis' storage

The full version of this doctoral thesis is stored at the office for Science and Research of Brno University of Technology Faculty of Electrical Engineering and Communication, Technická 3058/10, 616 00 Brno.

Místo uložení práce

Dizertační práce je uložena na oddělení Vědy a Výzkumu Fakulty Elektrotechniky a Komunikačních Technologií VUT v Brně, Technická 3058/10, 616 00 Brno.

Bibliographic citation

KUPAROWITZ, T. Charge transport and storage in a supercapacitor structure. Brno: Brno University of Technology, The Faculty of Electrical Engineering and Communication, 2017. 110 p. Supervisor doc. Ing. Petr Sedlak, Ph.D..

Bibliografická citace

KUPAROWITZ, T. Transport a ukládání náboje ve struktuře superkondenzátoru . Brno: Vysoké učení technické v Brně, Fakulta elektrotechniky a komunikačních technologií, 2017. 110 s. Vedoucí dizertační práce doc. Ing. Petr Sedlák, Ph.D..

Content

1 INTRODUCTION....1

2 STATE OF THE ART....2

2.1 Supercapacitor relaxation, restoration, and steady state voltage....2
2.2 Supercapacitor's parameters degradation....3
2.3 Helmholtz and diffuse capacitance....4

3 EVALUATED SC SAMPLES....5

4 SUPERCAPACITOR'S ELECTRIC CHARGE AND ENERGY....6

4.1 drift and diffusion in supercapacitor....6
4.2 Voltage relaxation and restoration....6
4.3 Supercapacitor relaxation dominant current component....8
4.4 Voltage dependent capacitance....10
4.5 Reciprocal capacitance and effective depletion region thickness....11
4.5.1 Reciprocal capacitance and effective depletion region thickness experiment....11

5 PROPOSED SC EQUIVALENT CIRCUIT MODEL....14

5.1 Helmholtz capacitance....15
5.2 Diffuse capacitance....15
5.3 Resistance between the Helmholtz and the diffuse capacitance....16
5.4 Equivalent series resistance....17
5.5 Leakage resistance....18
5.6 Reliability assessment....18

6 ACCELERATED AGING AND ITS INFLUENCE ON THE EQUIVALENT-CIRCUIT MODEL....19

6.1 Energy cycling tests....19
6.2 Calendar life tests....23
6.3 Effect of temperature and variable electric field on degradation of capacitance....24
6.4 Aging summary....24
6.4.1 Influence of sustained electric field....24
6.4.2 Influence of temperature....25

7 CONCLUSION....26

8 REFERENCES....27

9 AUTHOR'S CURRICULUM VITAE....28

10 ABSTRACT....30

1 INTRODUCTION

Supercapacitor (SC), a.k.a. ultracapacitor or electric double-layer capacitor, represents an electrical energy device, which offers high power density, short charging time, high number of charging cycles, and long-life duration. This device is of particular interest in fast energy-storage applications, where highly dynamic charging and discharging profiles with high current rates are required.

The gravimetric energy density of SC is gradually increasing with research and new technologies in this field. The energy density of lithium battery has been surpassed by that of SC in this decade. Further, it is projected to grow in conjunction with SC's reliability and market demand. These assumptions make SC industry very commercially appealing with projected growth of roughly nine fold in this decade.

SCs found an application in automotive industry (namely for inducing brief current surges during the engine start), in storing of harvested energy for autonomous sensor nodes, or in consumer electronics such as laptops or hand-held devices. SCs are used in combination with rechargeable batteries as power buffers and inside uninterruptible power supplies, where they replace stocks of electrolytic capacitors, reducing the size of the device, and increasing its cost effectiveness. Other use of SCs is in photo-voltaic and wind power systems, as power grid storage devices and voltage stabilizers. Knowledge, gained from learning SC's principles, finds its place in a new generation of rechargeable battery designs.

The concept of double-layer capacitance was first described in 1853. Despite that, the lack of understanding of their operation prevents to take full advantage of these devices. Several phenomena (e.g. voltage dependent capacitance, charge redistribution, voltage relaxation and restoration, performance fading, and the problem of creating physically appropriate model of SC) remain the subject of wide research.

The intention of this dissertation is to study the aforementioned phenomena occurring in SCs. Detailed study and modeling of the electrical charge transport and its storage is the output of this work. New equivalent electrical circuit model of SC is also proposed. Processes, which occur during charging and discharging, are studied and their correlation to fading of SC's parameters is assessed.

2 STATE OF THE ART

A model, describing the behavior of SC's (a.k.a. electrochemical double layer capacitor's) terminal voltage dependence on applied electric charge, is required for power electronics applications [1]. The first method, using a simple resistive-capacitive model (series RC circuit), showed that this approach is insufficient.

Zubieta and Bonert [1] propose an equivalent circuit to describe the measured terminal behavior of SC. This model is able to follow measured SC characteristics more precisely. The reason why the traditional models, used to describe capacitor behavior during charging/discharging, are inadequate for electrochemical double layer capacitors are discussed by many authors e.g. F. Rafik, et al. [2], or P. Sharma and T. S. Bhatti [3].

As it is known, SC can hold large amount of charge. It can be charged very quickly to high levels. But after that the susceptibility to being charged decreases rapidly and it is very hard to push any more additional charge into SC, even though its full capacitance potential has not been exceeded. In order to charge SC fully, time of the order of days [4]–[6] is needed. The same thing in reverse applies for the discharging. Thus, a considerable amount of charge always remains stored inside the SC during its normal use, even after fast discharge [5].

2.1 SUPERCAPACITOR RELAXATION, RESTORATION, AND STEADY STATE VOLTAGE

The SC relaxation is a process during which the terminal voltage of SC drops in time immediately after its charging stops. Assume an experiment, where there is a SC and a conventional capacitor of the same capacitance charged by constant voltage source. Both samples are completely discharged prior to the experiment. The charging is halted immediately, after the operating/rated voltage (V_{op}) is reached, as shown in Fig. 2.1. Here the voltage evolution of the charging dependence is red.

The open circuit voltage dependence of conventional capacitor is depicted green in Fig. 2.1. It would slowly decline in time due to leakage current. This decline would ultimately stop, once the capacitor gets completely discharged.

SC also sustains a voltage change after the charging (blue line in Fig. 2.1). The leakage current of SC is of the order of several μA, as described in [7]. This voltage drop is therefore not produced solely by SC's self-discharge. The rate of voltage decline gradually levels, until it stops at a nonzero **steady state voltage**.

The open circuit voltage dependence of recently charged SC is called the SC **relaxation**. SC relaxes, until it reaches steady state, at which it exhibits the steady state voltage. Note, that the steady state voltage value differs, based on the previous charging profile. Even though the process of SC relaxation is sometimes thought to be a self-discharge (e.g. [8]), different process is actually at play. In fact, the SC does not discharge, it only redistributes its charge.

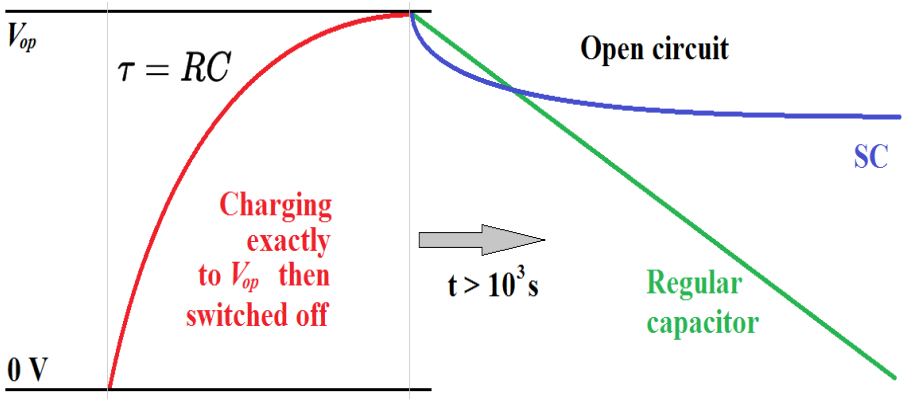

Fig. 2.1: Diagram of SC relaxation process (blue) and leakage of a conventional capacitor (green), after the charging by constant voltage source (red)

Similar, but quite the opposite process is the SC **restoration**. Here the terminal voltage (of previously charged SC) slowly increases after its abrupt discharge, until it reaches a steady state. This SC phenomenon is not well understood nor openly discussed in a contemporary science, but its existence is well acknowledged.

2.2 SUPERCAPACITOR'S PARAMETERS DEGRADATION

SC cells have porous activated carbon electrodes with high surface area. This and their inherent electrochemical inertness should in theory assure high power density (in comparison to batteries), high energy density (in comparison to capacitors), and an unlimited cycle life [9], [10]. The charge-storage and charge/discharge mechanisms of SC should therefore be highly reversible. But in practice the degradation of SC's performance is observed in a time frame of several months. This fading exhibits itself mainly in the form of decreasing capacitance [11].

Electrolyte’s chemical properties are deemed to play an important role in SC's degradation. It has been hypothesized, that impurities introduced to the electrode surface during manufacturing process are responsible for SC’s parameter fading. Reason being, that they block the active area of the electrode. Or, in the case of water, they stump the electrolyte. [12]–[14]

Various chemical processes in electrolyte itself could be responsible for parameter fading. Study of electrolyte decomposition reveals unwanted chemical reactions, that lead to hydrogen and carbon dioxide release [15], [16]. Destructive analysis of faded SC cells shows asymmetric changes in atomic composition of positive and negative electrodes [13]. In positive electrode the density of anions increases.

SC's parameter degradation also depends on the power level of operation and on the thermal environment of the device [7], [17], [18]. Regarding the voltage manufacturers contend that a permanent over-voltage of 0.1 V acts as a temperature increase of 10 °C. As [17] shows, both temperature and voltage should be taken into consideration while determining the degradation acceleration factor.

2.3 HELMHOLTZ AND DIFFUSE CAPACITANCE

It has long been established, that the voltage relaxation and restoration of SC are the products of diffusion like processes. These are well described by the Helmholtz theory. This theory (improved on by Gouy, Chapman, and Stern) permits to explain the different physical phenomena that occur at the interface between an ionic electrolyte and an electronic electrode. The interface is modeled by two superficial distributions of charges, the first one as electronic for the electrode, and the second one as ionic of opposed sign for the electrolyte. Even though it is demonstrable that these processes occur within SC, their concrete parameters, impact, and modeling are interpreted inconsistently among authors. Mainly the impact of SC aging has large influence on its change. The basic equations and description of Helmholtz processes are described below. [2], [3], [19], [20]

Helmholtz capacitance [4], [5], [19] is composed of thin layer at electrode/electrolyte interface. Electric charge stored in Helmholtz capacitance reacts immediately to the voltage change on electrodes. During charging by constant current, the voltage of SC’s electrodes does not increase linearly with time, as would be expected for regular parallel plate capacitor.

The voltage change on electrodes reacts with some time delay to change of electric charge distribution in depletion region, due to the motion of electric charge by diffusion. The region near the electrode has lower charge density due to the drift, which creates a charge gradient. This layer with lower charge density then fills slowly by charge from the bulk electrolyte. [19], [20]

The combination of both aforementioned principles has an influence on the distribution of charge in time during the charging process. Visualization of this effect

is presented in Fig. 2.2. Capacitance of SC is driven by the Helmholtz layer, consisting of charge stored at electrode/electrolyte interface, at first. The charge in electrolyte is assumed to be drifted by an electric field closer to the electrode/electrolyte interface. The drift produces a depletion region, into which the charge from bulk electrolyte diffuse.

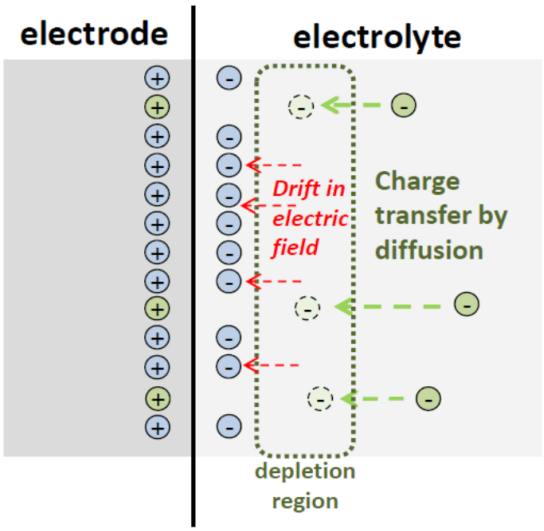

Fig. 2.2: Diagram of charge transfer in between Helmholtz and diffusion layers of SC [23]

3 EVALUATED SC SAMPLES

Three types of off-the-shelf SCs are analyzed in this thesis. All are relatively small issue and small capacitance SCs, designed to be used on printed circuit boards. It is assumed, that the underlying physical principles are common to all kinds of SCs. Samples with relatively low capacitance are therefore utilized for practical reasons, because the aging experiments may be performed faster.

1. Samples manufactured by Maxwell Technologies, Inc. (**Maxwell Technologies BCAP0010 P270 T01 10F 2.7V**) are referred to as samples SC Maxwell (2.7V/10F).
2. Samples **CapXX HS130 P2C361 2.40F 26mΩ 2.75V**, produced by CAP-XX Ltd., are referred to as SC CapXX (2.75V/2.4F) in this thesis.
3. SC Nesscap (2.7V/10F) is manufactured by Nesscap Ltd. company, under the designation **Ultracapacitor 2.7V / 10F ESHSR-0010C0-002R7**.

4 SUPERCAPACITOR'S ELECTRIC CHARGE AND ENERGY

This chapter deals with the description of inherent SC properties. It explains SC behavior and several SC phenomena. Relation between the change of stored charge, capacitance and change of terminal voltage for conventional capacitor is given by:

$$dQ = C\ dV \quad , \tag{1}$$

4.1 DRIFT AND DIFFUSION IN SUPERCAPACITOR

The change of the number of charge carriers near the Helmholtz layer may be quantified by linear differential equation:

$$dQ_H = Q_H \frac{dt}{\tau_H} \ , \tag{2}$$

Where dQ_H is the change of elementary charge count on Helmholtz double layer, Q_H is the charge on Helmholtz double layer, and τ_H is the time constant of this change.

For diffusion process, the movement of charge carriers does not follow linear pattern, but its speed is proportional to square root of time and the diffusion constant. The time dependence of elementary charge change dQ_D due to diffusion is:

$$dQ_D = \frac{Q_D dt}{2\sqrt{t \cdot \tau_D}} \ , \tag{3}$$

where Q_D is charge stored in diffusion layer and τ_D is its time constant.

4.2 VOLTAGE RELAXATION AND RESTORATION

It is assumed that both the process of SC relaxation, and the process of SC restoration are driven by the same underlying physical principle. Electric charge in SC is stored on electrodes as well as inside its electrolyte.

When a completely discharged SC gets charged (total charge $Q_T = I_c . \Delta t$ is injected), Helmholtz double layer is formed at its electrode/electrolyte interface by the drift of free charge carriers towards the opposite polarity electrode. It is said, that the Helmholtz double layer is being charged, even though only the electrode gets

external charge, and the charge within the electrolyte is redistributed. This process occurs immediately with a time constant of the order of seconds.

The resulting gradient of charge density allows for additional charge to diffuse toward the electrode from the electrolyte bulk. It is said, that the diffusion capacitance gets charged, while obviously only charge redistribution within the electrolyte occurs. This forms the diffusion capacitance, and it occurs with a time constant of the order of hundreds to thousands of seconds.

When a charged SC is briefly short-circuited (see Fig. 4.1), the Helmholtz double layer disintegrates. Charge on electrode is discharged entirely, however the state of charge in electrolyte remains mostly unchanged. The free charge carriers, stored near the opposite polarity electrodes (what used to be the Helmholtz layer), are then redistributed by diffusion back to the electrolyte. As the opposite polarity charge carriers slowly diffuse away from the electrode, SC's terminal voltage increases.

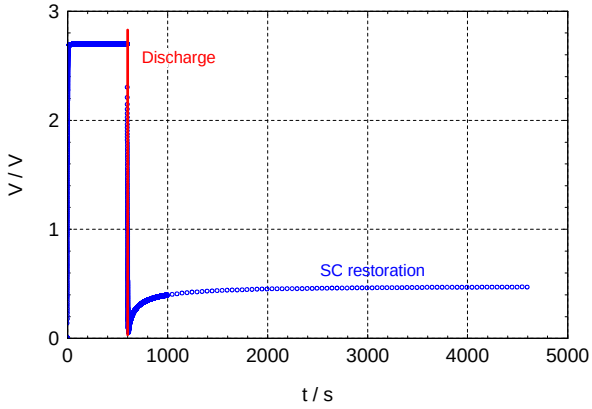

Fig. 4.1: Overview of full charging, short-circuit, and relaxation of SC

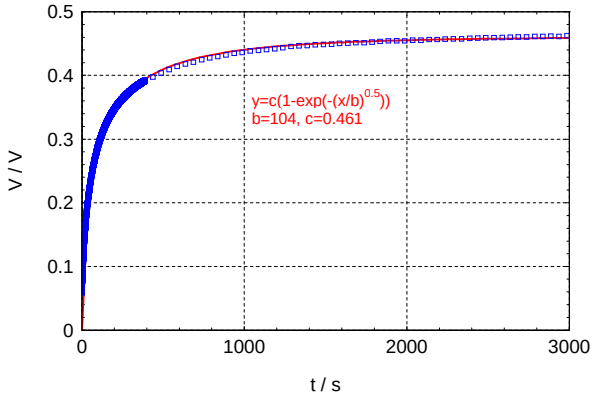

Fig. 4.2: Time dependence of voltage on SC's terminals (blue) and its fit (red) during the voltage recovery

It is safe to assume, that only the charge stored on electrodes was channeled out during the short-circuit (charge Q_d is channeled out). For C_T and Q_T it holds:

$$C_T = C_D + C_H \ , \ Q_T = Q_D + Q_H \ . \tag{4}$$

This allows for the approximation of the amount of charge stored in electrolyte $Q_D = Q_T - Q_d$. The Helmholtz capacitance is from (1) $C_H = Q_d / V_{op}$ and the total capacitance is $C_T = Q_T / V_{op}$.

Once the SC is shorted, charge Q_D is redistributed back to the electrodes (SC restoration) and the voltage on SC's terminals increases. The time dependence of

restoring voltage can be modeled by exponential stretched law (which shows that the charge redistribution is driven by diffusion process):

$$V = V_4\left(1-e^{-\sqrt{t/\tau_D}}\right) , \tag{5}$$

where V_4 is the restored SC's voltage at infinity, and τ_D is its time constant.

The experiment conclusively shows, that the electric charge of SC with carbon electrodes is stored not only in Helmholtz double layer (at the interface between the surface of a conductive electrode and an electrolyte), but also in the electrolyte itself.

4.3 SUPERCAPACITOR RELAXATION DOMINANT CURRENT COMPONENT

Helmholtz's theory states, that charge moves both by drift and by diffusion during the charging process (see chapter 2.3). Once the charging stops, so does the electric field applied to SC's terminals. The relaxation is driven mainly by charge diffusion. It may be safely modeled in that way for longer time intervals. Immediately after the charging ends however, the relaxation model must encompass both the diffusion current and the reversed drift current components. The ratio of diffusion current component and drift current component differs for different SCs. It's mainly influenced by the electrolyte composition.

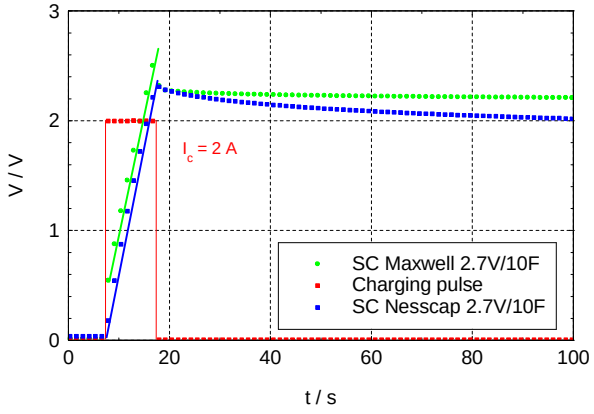

Fig. 4.3:SC Maxwell 2.7V/10F (green) and SC Nesscap 2.7V/10F (blue) charging and portion of subsequent relaxation

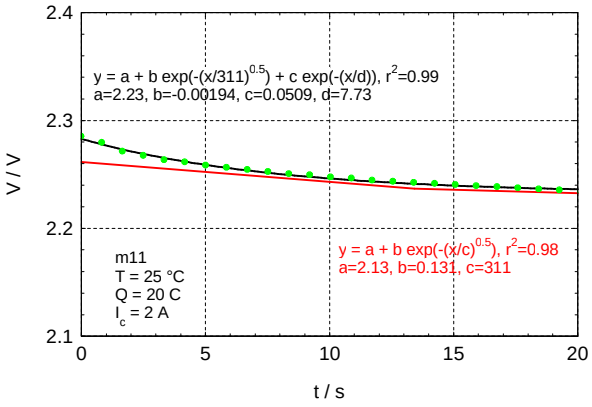

Fig. 4.4:SC Maxwell 2.7V/10F entire relaxation period (green) and its fit by analytical function based on diffusion (red) and accounting for drift (black)

The SC charged by constant current, and the process of relaxation is observed. First 100 s of this relation are depicted in Fig. 4.3 for samples of SC Maxwell and

SC Nesscap. The diffusion-driven process of SC relaxation is linked to exponential stretched law. It may be fitted by function derived from (3):

$$V = V_{2\infty} + \Delta V\, e^{-\sqrt{t/\tau_D}} \ , \tag{6}$$

where $V_{2\infty}$ is voltage at the end of the relaxation process, ΔV is voltage drop due to the relaxation, and τ_D is relaxation time constant.

In Fig. 4.4 a closeup of the first 20 s of the relaxation of SC Maxwell is shown. It is noticeable, that the data fit (red) does not properly cover the beginning of relaxation. This is due to the fact, that SC Maxwell has a high drift current component, which is dominant at the beginning of relaxation.

The beginning of relaxation is the combination of drift and diffusion processes:

$$V = V_2 + A e^{t/\tau_{dr}} + B e^{\sqrt{t/\tau_{df}}} \ . \tag{7}$$

where τ_{df} is time constant characterizing the diffusion process in the beginning of relaxation, τ_{dr} is time constant of drift process within the same interval, A and B are components that together produce the voltage drop ΔV at the end of drift current influence during the beginning of relaxation, and V_2 is SC's voltage at end of this time interval. (see Fig. 4.4.) It is assumed, that $\tau_{df} = \tau_D$ of the entire relaxation stretch.

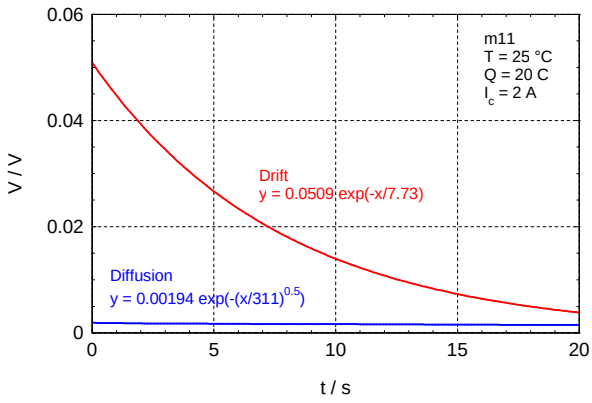

Fig. 4.5: SC Maxwell 2.7V/10F contribution of drift current component (red) and diffusion current component (blue) to the voltage change at the beginning of relaxation process

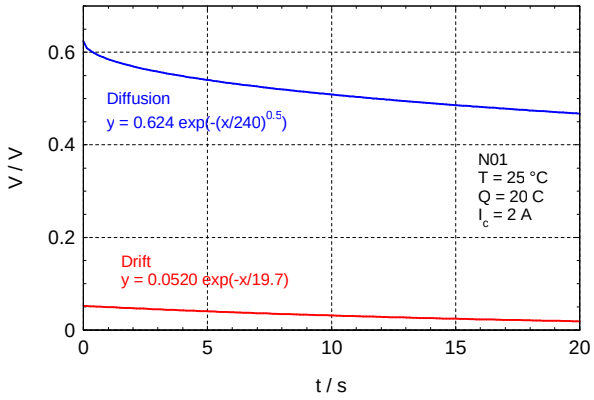

Fig. 4.6: SC Nesscap 2.7V/10F contribution of drift current component (red) and diffusion current component (blue) to the voltage change at the beginning of relaxation process

Figure 4.5 shows the ratio of drift and diffusion current processes of SC Maxwell 2.7V/10F. It is obvious, that the drift current has 10 times higher effect during the

beginning of SC relaxation. For SC Nesscap 2.7V/10F the ratio of drift and diffusion current components is depicted in Fig. 4.6. Here the diffusion current component has of the order of magnitude larger impact. The drift current component may therefore be neglected. The same as for SC Nesscap holds for SC CapXX. The drift current component must be accounted for while working with SCs that have it dominant, in order to model the beginning of relaxation properly.

4.4 VOLTAGE DEPENDENT CAPACITANCE

The physics of SC predicts a voltage dependent value of capacitance. This in practice means, that the value of its capacitance changes as does change its steady terminal voltage, as in Fig. 4.3. Note the characteristic bend of charging dependence. Blue lines represent the actual measured voltage dependencies for both utilized charging currents. These voltage curves are shifted to initiate at graph's origin. The charge transferred to the sample can be extrapolated in relation to its voltage on terminals.

.

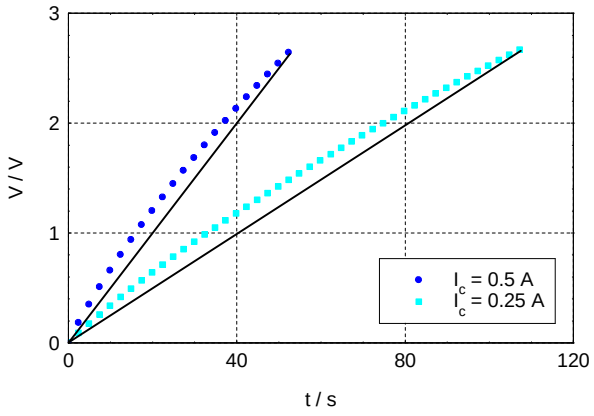

Fig. 4.7: Differential capacitance of SC for charging current 0.25 A (light blue) and 0.5 A (dark blue)

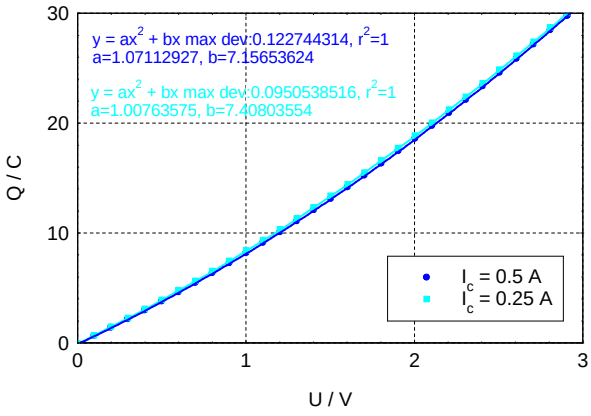

Fig. 4.8: Stored electric charge vs. voltage for charging by constant current 0.25 A (light blue), 0.5 A (dark blue) and its polynomial approximation

Electric charge in relation to potential could be approximated by 2nd order polynomial function:

$$Q = C_H V + \frac{1}{2} C_{H\delta} V^2 \ , \tag{8}$$

where C_H is Helmholtz capacitance and $C_{H\delta}$ is constant, which characterize voltage dependence of SC's capacitance.

Capacitance is, given by the first derivative of stored charge in relation to applied voltage (1). Hence it follows, that differential capacitance is linear with voltage:

$$C_{\delta} = C_{H} + C_{H\delta} V \quad . \tag{9}$$

The physical reason, why SC's capacitance depends on voltage and time, follows from the electric charge distribution in SC's active region. In parallel plate capacitor, the distance between positive and negative electric charge is constant, while in SC this distance is dependent on the electric field value and time. This happens because the charge moves between diffusion and Helmhotz layers. Distance between the positive and the negative charge decreases with increasing electric field and therefore SC's capacitance is a function of applied voltage and time. Mathematical method for obtaining capacitance estimation in relation to steady state voltage is described by (9).

4.5 RECIPROCAL CAPACITANCE AND EFFECTIVE DEPLETION REGION THICKNESS

This section explains the physical basis for charging duration dependence on its effective electrode thickness. Also the reciprocal capacitance concept is explained in this chapter. SC structure consists of two porous carbon based electrodes. The effective electrode area of evaluated samples is roughly A = 200 m^2. The space between electrodes is filled with an anion-rich electrolyte, and cellulose separator. The permittivity of the electrolyte turns out to be roughly $\varepsilon = 10^{10}$ F/m, and its work function is roughly 7 eV.

4.5.1 Reciprocal capacitance and effective depletion region thickness experiment

SC it is charged up to its V_{op} by a constant current pulse. Several different charging currents are employed, ranging from 0.5 A to 1 A, same as for differential capacitance evaluation in Fig. 4.7. The non-linear behavior of SC’s charging may be approximated by 2nd order polynomial function (9).Using (15) it follows, that SC’s reciprocal capacitance is $C^{-1} = V / Q$ shown in Fig. 4.9. This time dependence can be converted to dependence of stored charge.

SC’s effective depletion region thickness may be modeled through its reduction into system of single plate of parallel plate capacitor. This analogy fits well system with very slow charge movement, such as diffusion. For distance between electrodes

of parallel plate capacitor with constant concentration of ions in depletion layer it holds:

$$d = 2\varepsilon A C^{-1} \ , \tag{10}$$

where ε is electrolyte permittivity, d is distance between electrodes or thickness of depletion region, and A is the effective area of its electrode.

.

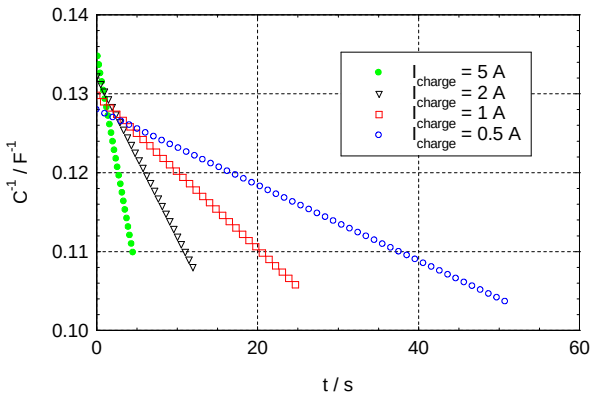

Fig. 4.9: Reciprocal capacitance of SC for varying currents vs time

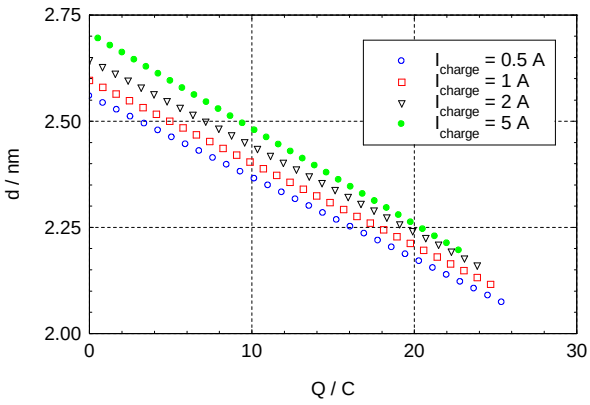

Fig. 4.10: Effective depletion layer thickness for varying currents vs relation to transferred charge

Relation of such effective depletion layer thickness is plotted in Fig. 4.10. From this figure it becomes obvious, that SC's effective depletion layer thickness is inversely proportional to both the amount of stored charge, and the charging duration. Note, that the effective depletion layer thickness is increased for higher charging currents (shorter charging duration).

It has been established, that the effective depletion layer thickness of SC changes. It happens both due to the amount of charge transferred into it, and due to the time the change takes. The effect of varying depletion layer thickness can be quantified using Gauss' law, as the integration of electric field over the electrode area:

$$\frac{Q}{\varepsilon} = \oint \vec{E} \cdot \vec{dA} \ , \tag{11}$$

where E is vector of electric field and dA is vector of increment of area, representing elementary area of the electrode surface. For electric field intensity, immediately at single electrode boundary, it therefore holds:

$$E_0 = \frac{\rho d}{\varepsilon} = \frac{e n A d}{\varepsilon A} = \frac{I \cdot t}{\varepsilon A} = \frac{e n A}{C} \quad , \tag{12}$$

where e is elementary charge and n is negative charge count. It must hold, that E_0 is countered by positive charge buildup on carbon electrode.

.

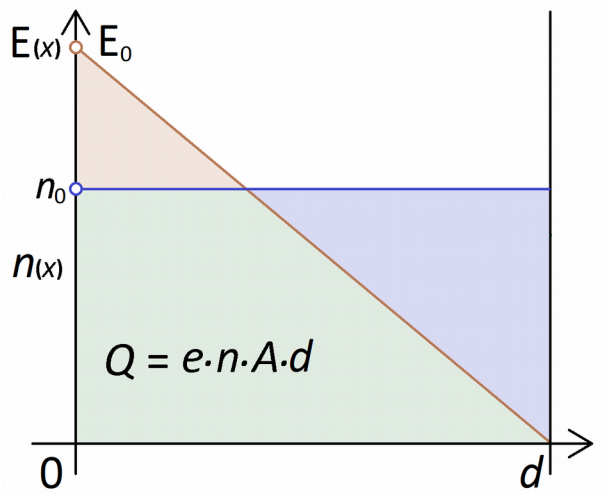

Fig. 4.11: Electric field dependence in electrolyte near carbon electrode for constant electric charge density

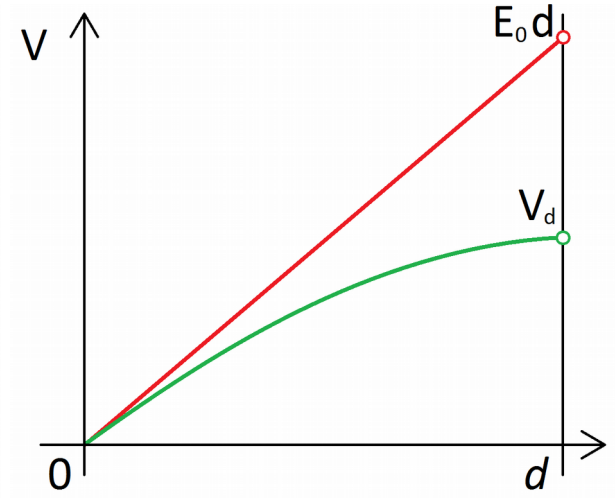

Fig. 4.12: Electric potential distribution in depletion region in relation to distance from single electrode for SC (green) and regular parallel plate capacitor (red)

In the beginning of the charging process, the electric field dependence in electrolyte in proximity to carbon/electrolyte interface is shown in Fig. 4.11 (brown line). Here the electric field intensity E_0 starts off immediately at the electrode and decreases with distance x, until it reaches zero at the end of electrolyte effective depletion region d. Electric charge density (blue line) is constant at SC steady state. The total charge within the depletion region is $Q = e.n.A.d$. For the evolution of electric field intensity with distance x it holds:

$$E(x) = \int \frac{\rho}{\varepsilon} dx = \frac{\rho}{\varepsilon} x \Big|_0^d = \frac{\rho}{\varepsilon}(d - x) = E_0\left(1 - \frac{x}{d}\right) \quad . \tag{13}$$

Integration of (13), with respect to distance from carbon electrode to the end of constant charge region, gives the relation of potential within electrolyte:

$$V(x) = \int_0^x E(x) dx = E_0 x - \frac{e \cdot n}{2\varepsilon} x^2 \quad . \tag{14}$$

The relation of potential distribution in relation to distance from capacitor electrode is depicted in figure above. The red curve represents potential distribution of parallel plate capacitor, which is only bound by the term $V(x) = E_0 x$ of (14).

The green curve of Fig. 4.12 represents the potential distribution inside SC with free moving charge carriers in close proximity to the electrode, as predicted by (14).

In other words, the relation of electric intensity over area, and the potential evolution within electrolyte are thus linked to unidirectional charge distribution around the opposite polarity electrode.

From the above findings it concludes, that the depth of the depletion region near carbon electrode is within 3 nm thick (see Fig. 4.10). This is of several orders of magnitude less, than the size of cavities of activated carbon electrode.

5 PROPOSED SC EQUIVALENT CIRCUIT MODEL

New 5 parameter SC equivalent electrical circuit model (ECM) is proposed. This model is simple and easy to utilize for SC's behavior estimation. It is constructed to reflect the underlying SC's physical properties. It has less then relative 5% error. Scheme of this model is shown in Fig. 5.1. [23]

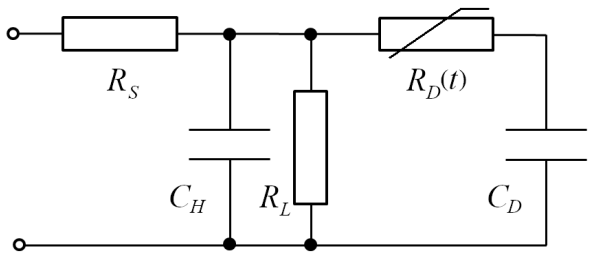

Fig. 5.1: Proposed equivalent electrical circuit model

All model parameters are retrieved using an analytical description from measurements of SC's terminal characteristics. To do so, the SC is charged by constant current pulse, after which the relaxation period is observed, same as for experiment in chapter 4.3 (see Fig. 4.3). Observation of 2000 s should be sufficient.

The I_c used should be at the upper boundary of SC's comfortable zone, in order to minimize the charge loss to the diffusion layer. On the other hand, the charging current must be low enough, in order not to induce any thermal effects in SC.

5.1 HELMHOLTZ CAPACITANCE

The SC's immediate capacitance, marked C_H in Fig. 5.1. After the charging interval, the voltage drop across SC's terminals is measured (see Fig. 5.2). This voltage characteristic could be fitted by (6).

Since the charging pulse is relatively brief, it may be assumed that only the Helmholtz capacitance is charged in this time interval, and that the charge transferred to the diffuse capacitance is negligible. This means, that at the end of the charging, the charge stored in Helmholtz capacitance is $Q_H = Q_T$. From (1) it then follows, that $C_H = Q_H / V_1$, where $V_1 = V_H$ is the SC's voltage at relaxation beginning.

An alternative method for C_H estimation would be the fitting of charging relation by equation 8. The value of C_H would then be the one obtained from (9).

5.2 DIFFUSE CAPACITANCE

Diffuse capacitance (designated C_D in Fig. 5.1) represents the ability of electrolyte to effectively hold charge. Such charge is held in a form of ions, that diffuse into the depletion region from the electrolyte bulk, after the charge drift occurs near the Helmholtz layer. Diffuse capacitance actually contributes to the overall capacitance of SC and it absorbs some of the total charge stored in SC.

Since both C_D and C_H are effectively in parallel, the charge in ECM transfers into C_D, until an equilibrium of potentials is reached. This is a manifestation of the SC relaxation process. During this the charge buildup on Helmholtz layer (by drift) creates a depletion region near the electrode. The drift of additional charge from electrolyte bulk decreases due to low electric field in larger distance from the electrode, as explained in chapter 4.5. This forms a depletion region characterized by lower electric charge concentration. Such depletion region has therefore a low charge density, which allows for the diffusion of charge into this region from within the electrolyte bulk (see Fig. 2.2). The incoming charge serves to counter the effect of charge stored on electrodes, reducing the overall electric field intensity, that the charge on electrode exerts. This has the effect of terminal voltage decrease.

When the voltage of C_H suddenly drops below the level of C_D (e.g. in the case of SC short-circuit), the diffuse capacitance slowly discharges itself through $R_D(t)$ into the Helmholtz one. This is observed as SC restoration on its terminals. It is a result of previously drifted charge not being held at Helmholtz double-layer anymore. The charge density near the electrode increases suddenly, which leads to its diffusion into

the electrolyte bulk. This process is the opposite to the one described in paragraph above.

Taking into consideration the overall SC capacitance and the Helmholtz capacitance; the value of diffuse capacitance is from (4):

$$C_D = C_T - C_H = Q_T/V_{2\infty} - Q_H/V_1 \ . \tag{15}$$

Same as for Helmholtz capacitance, both the total and diffuse capacitances could be evaluated more precisely using method described in chapter 4.4.

.

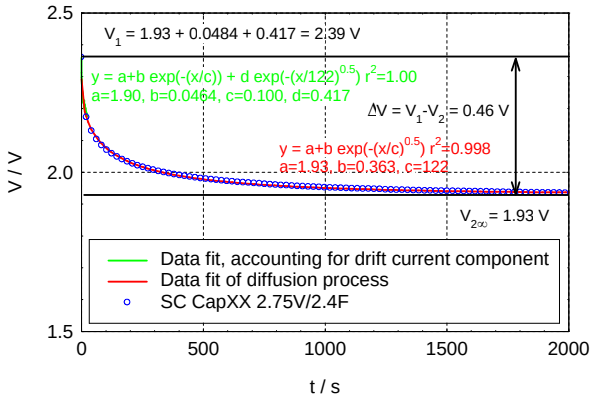

Fig. 5.2: SC Maxwell voltage relaxation (blue), data fit by analytical function accounting for diffusion process (red), and data fit by analytical function accounting for drift process at the beginning of SC relaxation (green)

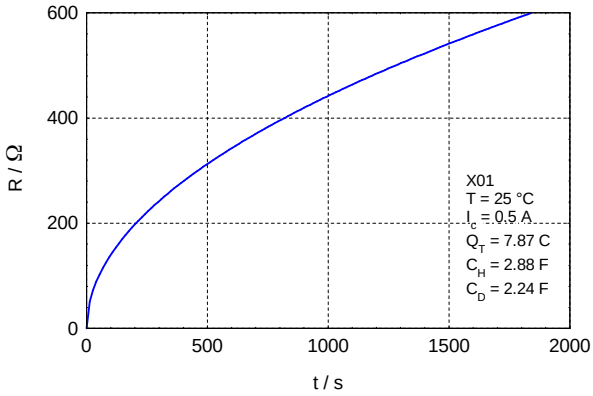

Fig. 5.3:SC CapXX 2.75V/2.4F time dependent resistance solved analytically

5.3 RESISTANCE BETWEEN THE HELMHOLTZ AND THE DIFFUSE CAPACITANCE

This variable resistance ($R_D(t)$ in Fig. 5.1) represents the decreasing probability of another charge carriers' transport by diffusion. SC relaxation is discussed in this thesis, but the same process is applicable in reverse for SC restoration (disregarding the drift component, as there is no electrical field applied).

Considering the Helmholtz capacitance to be constant, following is true for charge stored at Q_D from (6):

$$Q_D = Q_{D\infty}\left(1 - e^{-\sqrt{t/\tau_D}}\right) \ , \tag{16}$$

where $Q_{D\infty}$ is charge stored on C_D once the diffusion process has finished and τ_D is time constant of the relaxation process.

The charge transfer between Q_H and Q_D in time (considering that Q_T remains constant) can be expressed in a form of diffuse current, flowing from C_H to C_D:

$$I_D = \frac{dQ_D}{dt} = Q_{D\infty} \frac{e^{-\sqrt{\frac{t}{\tau_D}}}}{2\tau_D \sqrt{\frac{t}{\tau_D}}} = I_{D\infty} \frac{e^{-\sqrt{\frac{t}{\tau_D}}}}{\sqrt{\frac{t}{\tau_D}}} \ , \tag{17}$$

where dQ_D is change in diffusion layer charge, and $I_{D\infty} = Q_{D\infty} / 2\tau_D$ is diffuse current constant. For the time dependent resistance between Helmholtz and diffusion layer it holds from Ohm's law:

$$R_D(t) = \frac{V_H - V_D}{I_D(t)} \ . \tag{18}$$

For scenario, where the SC was fully discharged prior to the measurement, following relation is obtained from (18):

$$R_D(t) = \frac{V_H}{I_{D\infty}} \sqrt{t/\tau_D} = \frac{2\tau_D V_H}{Q_{D\infty}} \sqrt{t/\tau_D} = 2\frac{V_H \sqrt{\tau_D}}{C_D V_{2\infty}} \sqrt{t} = R_{D1} \sqrt{t} \ , \tag{19}$$

where R_{D1} is diffuse resistance parameter constant, showing the resistance value at time 1 s. The value of R_{D1}, characterizing the diffusion resistance $R_D(t)$, is then:

$$R_{D1} = 2\frac{V_H \sqrt{\tau_D}}{C_D V_{2\infty}} \ . \tag{20}$$

An evolution of the value $R_D(t)$ during relaxation is depicted in Fig. 5.3.

5.4 EQUIVALENT SERIES RESISTANCE

Resistance R_S represents the DC ESR of SC in ECM, as depicted in Fig. 5.1. It is produced by the resistance of leads and the carbon electrode, and by electrolyte conductivity. Value of SC's ESR may most easily be acquired from voltage step ΔV_{ESR}, which occurs when the magnitude of DC current through the SC changes. The value is then from Ohm's law $R_S = \Delta V_{ESR} / I_c$.

5.5 LEAKAGE RESISTANCE

The leakage resistance R_L is directly proportional to SC's leakage current and the steady state voltage. This parameter is situated parallel to C_H in ECM. In order to evaluate the leakage resistance precisely, method published in [7] may be used. In ECM the value R_L in range from 10 kΩ to 1 MΩ could be successfully utilized.

5.6 RELIABILITY ASSESSMENT

ECM omits drift processes, which causes in the worst case scenario an absolute error of 0.1 V for fully charged capacitor. The relative error is however below 5% for the entire measurement. For longer time intervals (over 500 s) the relative difference between the experiment and the simulation is below 0.5%. The accuracy of ECM is evaluated based on its empirical probability. This represents the ratio of the number of outcomes in which a specified event occurs, to the total number of trials. [23]

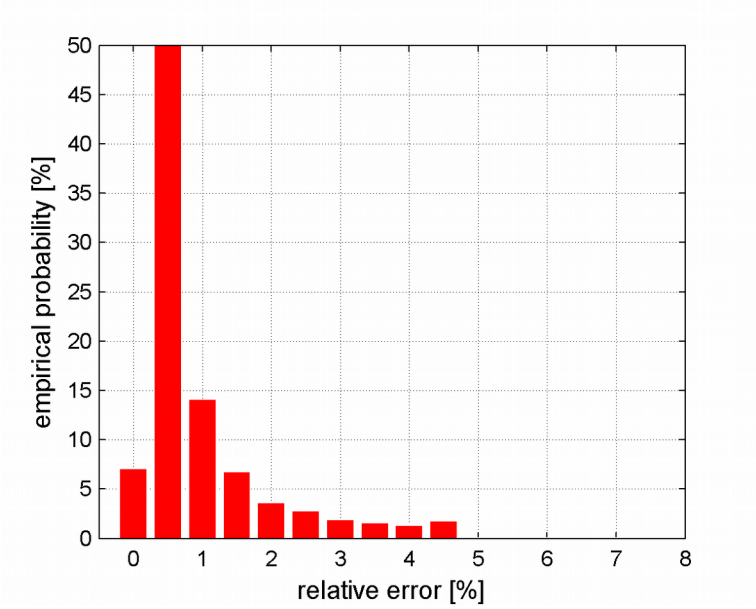

Fig. 5.4: The dependence of empirical probability on relative error between simulation results of equivalent circuit model and experimental data [23]

Fig. 5.4 shows the dependence of empirical probability in comparison to the relative error of simulation compared to the actual measurement. For ECM more than 70% of monitored interval is within the 1% relative error margin. For the rest of the monitored interval the relative error always remains under 5%.

6 ACCELERATED AGING AND ITS INFLUENCE ON THE EQUIVALENT-CIRCUIT MODEL

This chapter pursues the analysis of SC aging. As stated before, SC should in theory have infinite cycle life, due to the electrochemical inertness of its main components. In practice though, the state of health of SC, which is manifested through the degradation of its ECM parameters, is strongly dependent on the abuse SC sustains throughout its lifetime. Such an abuse may be inflicted on SC by several different means, which all stem from the expected kinds of usage of said device.

Firstly, the effect of charge transport during charging/discharging must be considered. Next thing to account for is the effect of temperature, which may either be of environmental source or a Joule's heat produced by charging/discharging currents. The last studied manner of degradation is the effect of keeping SC at constant voltage within varying ambient temperature.

In order to artificially inflict the kind of damage SC sustains during its normal operation, several experimental methods are devised to test it. These methods are based on SC's basic work profile during its actual deployment. Two general kinds of methods are employed and presented: energy cycling tests and the calendar life tests.

6.1 ENERGY CYCLING TESTS

This family of induced aging methods is based on cyclic charging and discharging of studied SC samples. Such processes alter the relative amount of energy stored within tested SC. Energy stored in conventional capacitor in relation to its terminal voltage is given by the equation:

$$E = \frac{1}{2} C V^2 \ , \tag{21}$$

where E stands for stored energy, C is its capacitance, and V is terminal voltage.

Energy cycling tests are based on periodic constant current charge pulses up to SC's operating voltage V_{op} during every cycle. It then must be discharged back to 0 V in order for 100% of the energy to shift in and out. Or (from (21)) back to ½ V_{op} to shift 75% of stored energy in and out of the sample.

The depreciation of SC's parameters (due to energy cycling tests) is evaluated in relation to both, the total duration of these tests in hours, and the total number n of

endured test cycles. Parameters are evaluated every 10^5 cycles. Following ECM parameters are analyzed: C_T, C_H, C_D, τ_D, R_S, and R_{D1}. In addition, a conventional DC capacitance (C_{DC}) and DC ESR (R_{DC}), are evaluated using an RLC Meter.

Continuous energy cycling (CEC) comprises discharging by constant current (I_d), followed immediately by charging, which constitutes a single test cycle. These are 75% and 100% CEC. Diagram of an expected voltage dependence of an ideal capacitor is depicted in Fig. 6.1. The value of $I_c = I_d = 2.7$ A is selected for both CEC methods. The effect of self-heating may therefore be neglected in comparison.

.

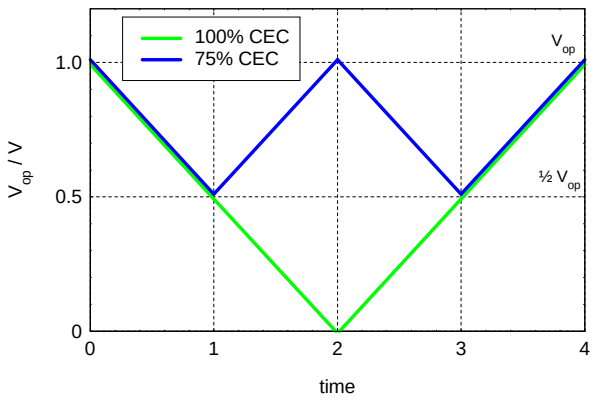

Fig. 6.1: Diagram of SC's voltage dependence for 100% energy cycling test (green) and 75% energy cycling test (blue)

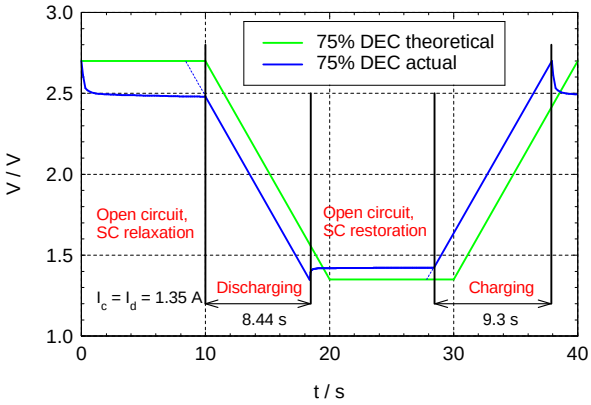

Fig. 6.2: Diagram of SC's voltage dependence for single cycle of 75% discontinuous energy cycling test; theoretical (green) and actual (blue) dependence

Discontinuous energy cycling (DEC) is essentially the same as CEC, with the only difference being an additional time interval after each charging and discharging segments, while the SC remains in open circuit condition. It is devised to simulate sporadic load profile of SC. Only the 75% DEC variant of this test is presented.

Charging and discharging currents are again the same $I_c = I_d = 1.35$ A. Note, that within the dead time period, the diffuse capacitance of sample gets charged (SC relaxation) or discharged (SC restoration) gradually, as shown in Fig. 6.2. Such voltage shift results in shortening of the charging and discharging periods. Sample's temperature increases by ~ 8 °C as a result of 75% DEC test at 1.35 A.

First explored SC parameter is the total capacitance. In tables above it is presented as a conventional DC capacitance C_{DC}, measured by an LRC meter, and the C_T,

which may be obtained using (4). The change of total capacitance in relation to the number of energy cycling aging cycles n follows an exponential stretched law:

$$C(n) = C_{\infty} + \Delta C\, e^{-\sqrt{\frac{n}{n_{EC}}}}\ ,\ C(t) = C_{\infty} + \Delta C\, e^{-\sqrt{\frac{t}{\tau_{EC}}}}\ , \qquad (22)$$

where C_{∞} is expected capacitance value at infinity, ΔC is the drop of capacitance due to aging, and n_{EC} is the constant, which characterizes the capacitance degradation in number of endured charging cycles, and τ_{EC} is the time constant of aging process.

Equations (22) hold for the change of C_T and C_{DC} for roughly 2000 hours of CEC aging by current 2.7 A. After that the capacitance decrease becomes linear. This linear drop-off (see Fig. 6.3) is an indicator of looming SC failure, and it initiates after the capacitance decreases by ~20%, depending on the temperature.

.

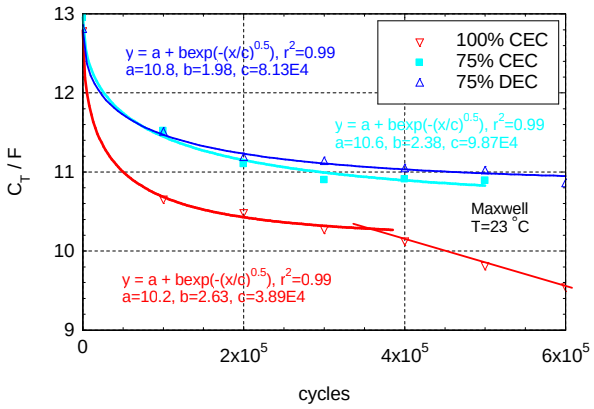

Fig. 6.3: Change of total capacitance of SC Maxwell 10F/2.7V in relation to energy cycling

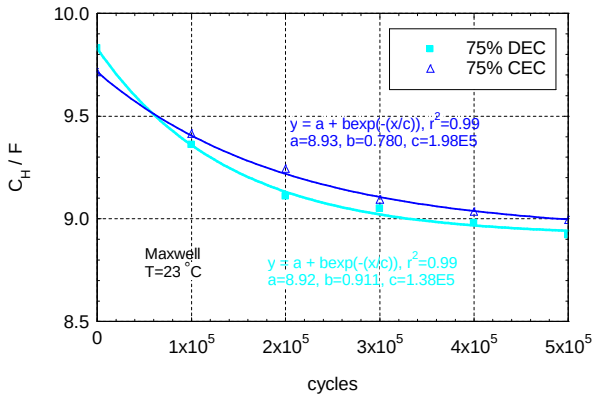

Fig. 6.4: Change of Helmholtz capacitance of SC Maxwell 10F/2.7V in relation to energy cycling

While the evolution of total capacitance depends on the square root of time, the change of Helmholtz capacitance may be described most accurately by a pure exponential function. It is so, because the Helmholtz capacitance's behavior is mostly influenced by the fast motion of charge at the electrode/electrolyte interface by drift, and therefore does not succumb to diffusion like behavior. The capacitance then drops exponentially, as the effective electrode area decreases linearly by physical aggravation, induced by varying electric field.

Fig. 6.4 shows the decrease of Helmholtz capacitance. Again, the capacitance drops suddenly after 2000 hours due to induced Joule's heat. This drop occurs earlier

with SC Maxwell than with SC Nesscap. The decrease of Helmholtz capacitance is in turn faster for SC Nesscap.

The value of diffuse capacitance C_D decreases sharply due to aging at first. It follows an exponential decline, which is induced by the polarization of electrolyte within its first use. This decline happens within the first or up to the second aging round so it is not clearly visible in presented data (it may be approximated by line).

.

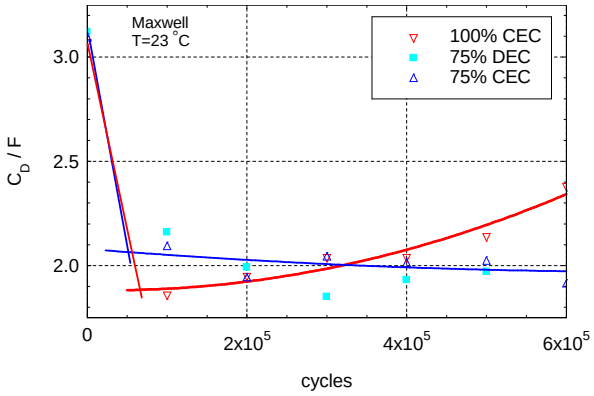

Fig. 6.5: Change of diffuse capacitance of SC Maxwell 10F/2.7V in relation to energy cycling

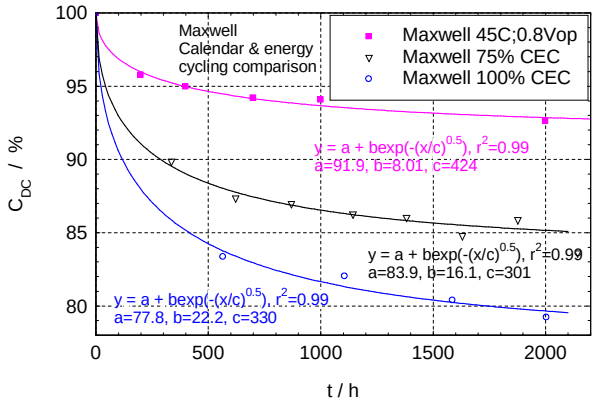

Fig. 6.6: Comparison of influence of different aging methods on the change of DC capacitance

After the sharp exponential decline, the diffuse capacitance starts to behave quadratically, slowly decreasing at first, as shown in Fig. 6.5. After additional cycling it starts to slowly grow. This behavior is the same for both types of SC.

The electrolyte degradation is responsible for change of diffuse capacitance. As its permittivity decreases, so does the capacitance at first. This is induced by the integration of opposite polarity dipoles within the electrolyte.

The change of ECM resistance between Helmholtz and diffuse capacitances $R_D(t)$ is presented by its diffusion resistance constant R_{D1}. Neither studied SC is notably affected by the heat induced by aging. The dependency of diffuse resistance $R_D(t)$ is expressed by its parameter R_{D1}. For SC Nesscap is the aging of R_{D1} governed by:

$$R(n) = R_0 + \Delta R\left(1 - e^{-\sqrt{\frac{n}{n_{EC}}}}\right), \quad R(t) = R_0 + \Delta R\left(1 - e^{-\sqrt{\frac{t}{\tau_{EC}}}}\right), \tag{23}$$

where R_0 is the original value of resistance and ΔR is its increase due to aging.

The increase of R_{D1} shows, that with aging it is increasingly harder for the diffusion layer to charge.

Both the ECM ESR (R_S) and the DC ESR, measured using conventional LRC meter, increase quadratically in time with aging. The rate of ESR change differs proportionally to percentage of CEC method implored, suggesting that the change of the value depends on electric field. This means that higher energy method used has a detrimental effect on series resistance, and that the temperature has low effect.

6.2 CALENDAR LIFE TESTS

Calendar life tests are devised to simulate SC under light work load at differing ambient temperatures ranging from -35 °C up to 65 °C. In this test, the stored energy of SC is sustained by maintaining the voltage at a constant value for long time period (over 11 000 hours). The range of applied voltages is for different experiments from 0.6xV_{op} to 1.2xV_{op} (this means overcharging the SC).

Calendar life tests of SC Nesscap produce DC capacitance change (obtained using an LRC meter) presented in Fig. 6.7. Data are transformed to their relative change in percents. First thing to notice is that the capacitance decrease is proportional to applied temperature. Second thing is the detrimental effect of SC overcharging at temperatures higher then the room temperature.

.

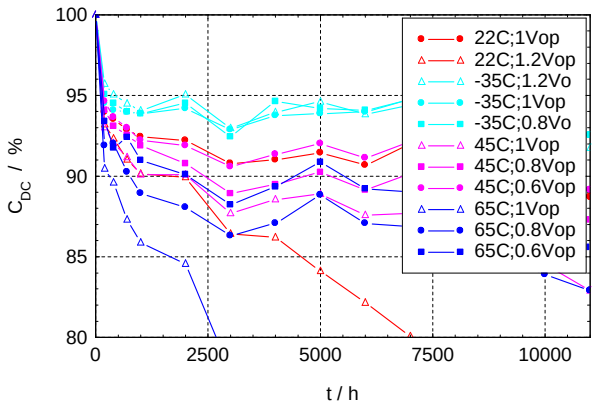

Fig. 6.7: Change of relative capacitance during calendar life tests for varying temperatures and applied voltage

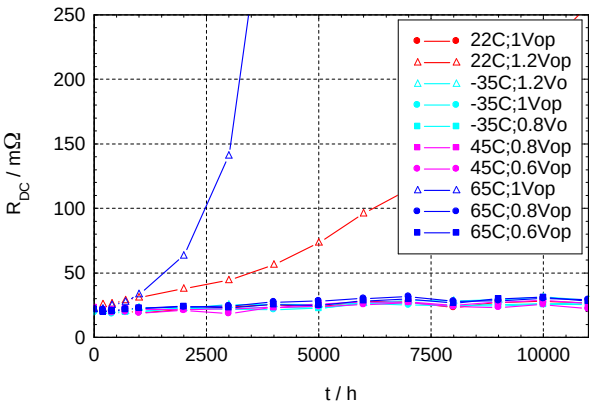

Fig. 6.8: Change of DC resistance during calendar life tests for varying temperatures and applied voltage

The DC resistance in relation to calendar life tests for SC Nesscap is presented in Fig. 6.8. Note, that its value does not decline solely due to the temperature. It only

significantly increases for samples that are on the verge of malfunctioning, such as the overheated (blue triangle) and overcharged (red triangle) dependencies.

6.3 EFFECT OF TEMPERATURE AND VARIABLE ELECTRIC FIELD ON DEGRADATION OF CAPACITANCE

The effect of energy cycling and calendar life tests on capacitance is assessed. The aim is to figure out if self-heating could lead to different depreciation processes than those of varying electric field.

The temperature increase of SC due to CEC at 2.7 A is roughly 20 °C. If the only source of SC's capacitance degradation is the increased temperature, the capacitance evolution for CEC methods should overlap with appropriate life cycling one. The 75% and 100% CEC methods should correspond to the 0.75 V_{op} and 0.5 V_{op} calendar life tests at temperature 42 °C, respectively. The worst case scenario of 0.8 Vop at 45 °C, is compared to the capacitance decrease of CEC methods in Fig. 6.6 above.

From Fig. 6.6 it follows, that the total capacitance depreciation must also be dependent on transferred charge. Note, that all relations in presented plots obey the equation (22). From its data fit it is clear, that SC looses ~8% of capacitance as a result of increased temperature, and additional ~8% or ~14% of capacitance due to energy cycling for 75% CEC or 100% CEC, respectively. Hence the impact of variable electric field must be taken into account as an additional source of capacitance degradation.

6.4 AGING SUMMARY

Two main variables seem to affect the SC's degradation. These are the effect of sustained electric field and the effect of temperature.

6.4.1 Influence of sustained electric field

The application of electric field to SC results in the polarization of its electrolyte within short time span. Once the field dissipates, the free ions are allowed to move around by diffusion like processes. This results in the clogging of electrode surface by impurities. The decrease of electrode effective area is thus linear. This results in:

1. Smaller value of Helmholtz capacitance, which decreases exponentially. This is the main reason why 75% DEC produces larger capacitance decrease than the 100% CEC aging method. This difference is most noticeable for SC

Nesscap and SC CapXX, which have a high diffusion current component, meaning that the electrolyte composition is inferior to that of SC Maxwell in this aspect.

2. And larger value of series resistance, which is quadratic. This is why both 75% energy cycling tests produce the same ESR increase. The ESR increase is generally smaller for SC Nesscap than for SC Maxwell. The higher value of ESR for SC Maxwell is also due to the difference in electrolyte's conductivity.

The change of applied electric field produces changes in electrolyte. These changes are most notably manifested through:

1. Electrolyte's polarization within the applied electric field. Resulting (among others) in its conductivity increase, which is much more profound for SC Nesscap and SC CapXX. This has an influence on SC's ESR change.

2. Permittivity decrease, once the electric field dissipates. This is produced gradually, once the polarized electrolyte recombines back to its original state. This recombination is an electrochemical reaction, and as such its reproducibility is not 100%. This results in reduction of ions, that can participate in diffusion capacitance charging.

3. Another result of electrolyte change due to sustained electric field is the impediment of diffusion process time constant (τ_D) decline.

The amount of charge that shifts in and out of SC is responsible for the speed of SC's depreciation. With increasing amount of transferred charge, the total capacitance C_T or C_{DC} fades faster during energy cycling. Such speed may be described by the means of n_{EC} and τ_{EC} from (22). With increasing amount of transferred charge, the rate of total capacitance depreciation increases. The depreciation of the value of total capacitance itself is then mostly dependent on the value of applied electric field and sample's temperature. After a sufficient (temperature dependent) capacitance decline, its value starts to drop-off linearly.

6.4.2 Influence of temperature

The rate of SC's parameters decline is also dependent on its operating temperature. This can be either the ambient temperature or the one induced by Joule's heat. The increased temperature generally promotes chemical reactions, that occur in electrolyte. After a certain (temperature dependent) time, SC's parameters

start to fail rapidly. This noticeable change signals the half of SC's life, under sustained conditions.

For SC with electric field equal to its V_{op} applied, this halftime is roughly 4000 h to 8000 h at room temperature; 2000 h to 4000 h at 45 °C; and below 2000 hours at 65 °C. As can be seen, SC generally operates better at lower temperatures. After this failure, the total capacitance, Helmholtz capacitance, and diffusion time constant of SC decline linearly until the SC malfunctions.

7 CONCLUSION

The study of charge transport in supercapacitor's (SC's) diffuse layer was performed. This layer is responsible for SC relaxation after charging, and SC restoration after a fast discharge. The time dependence of diffuse and drift current components of electrolytes for different manufacturers are described. SC Maxwell has a high drift current component, while SC Nesscap and SC CapXX have high diffuse current component.

The phenomenon of SC's voltage dependent capacitance is assessed. Analytical function, which describes it in relation to SC's steady state voltage, is proposed.

SC's effective depletion layer thickness is assessed for varying magnitudes of charging currents. Its thickness decreases linearly with the charge transferred to SC. It changes from 2.75 nm to 2.1 nm. The thickness is of several orders of magnitude less, then the size of activated carbon cavities.

New SC's equivalent circuit model (ECM) is constructed. It reflects the underlying physical properties of SC. The model consists of Helmholtz capacitance, diffuse capacitance, equivalent series resistance, leakage resistance, and time dependent resistance, which represents the decreasing likelihood of another charge carrier to participate in the diffusion process. This model is described in chapter 5.

Two methods of accelerated SC aging are presented; these are 1) the continuous (CEC) and discontinuous (DEC) energy cycling tests, and 2) the calendar life tests. Aging of SCs is performed, during which their parameters are periodically evaluated. The findings, related to such parameter's change, are summarized in chapter 6.4.

8 REFERENCES

[1] L. Zubieta and R. Bonert, “Characterization of double-layer capacitors for power electronics applications,” *IEEE Trans. Ind. Appl.*, vol. 36, no. 1, pp. 199–205, Jan. 2000.

[2] F. Rafik, H. Gualous, R. Gallay, A. Crausaz, and A. Berthon, “Frequency, thermal and voltage supercapacitor characterization and modeling,” *J. Power Sources*, vol. 165, no. 2, pp. 928–934, Mar. 2007.

[3] P. Sharma and T. S. Bhatti, “A review on electrochemical double-layer capacitors,” *Energy Convers. Manag.*, vol. 51, no. 12, pp. 2901–2912, Dec. 2010.

[4] D. Torregrossa, M. Bahramipanah, E. Namor, R. Cherkaoui, and M. Paolone, “Improvement of Dynamic Modeling of Supercapacitor by Residual Charge Effect Estimation,” *IEEE Trans. Ind. Electron.*, vol. 61, no. 3, pp. 1345–1354, Mar. 2014.

[5] M. Kaus, J. Kowal, and D. U. Sauer, “Modelling the effects of charge redistribution during self-discharge of supercapacitors,” *Electrochimica Acta*, vol. 55, no. 25, pp. 7516–7523, Oct. 2010.

[6] J. W. Graydon, M. Panjehshahi, and D. W. Kirk, “Charge redistribution and ionic mobility in the micropores of supercapacitors,” *J. Power Sources*, vol. 245, pp. 822–829, Jan. 2014.

[7] Vlasta Sedlakova, Josef Sikula, Juraj Valsa, Jiri Majzner, and Petr Dvorak, “Supercapacitor charge and self-discharge analysis,” in *Proceedings of conference Passive Space Component Days*, Noordwijk, The Netherlands, 2013.

[8] H. El Brouji, J.-M. Vinassa, O. Briat, N. Bertrand, and E. Woirgard, “Ultracapacitors self discharge modelling using a physical description of porous electrode impedance,” in *IEEE Vehicle Power and Propulsion Conference, 2008. VPPC ’08*, 2008, pp. 1–6.

[9] B. E. Conway, *Electrochemical supercapacitors: scientific fundamentals and technological applications*. New York: Plenum Press, 1999.

[10] E.-H. El Brouji, O. Briat, J.-M. Vinassa, N. Bertrand, and E. Woirgard, “Impact of Calendar Life and Cycling Ageing on Supercapacitor Performance,” *IEEE Trans. Veh. Technol.*, vol. 58, no. 8, pp. 3917–3929, Oct. 2009.

[11] T. Umemura, Y. Mizutani, T. Okamoto, T. Taguchi, K. Nakajima, and K. Tanaka, “Life expectancy and degradation behavior of electric double layer capacitor part I,” in *Proceedings of the 7th International Conference on Properties and Applications of Dielectric Materials, 2003*, 2003, vol. 3, pp. 944–948 vol.3.

[12] V. Ruiz, C. Blanco, M. Granda, and R. Santamaría, “Enhanced life-cycle supercapacitors by thermal treatment of mesophase-derived activated carbons,” *Electrochimica Acta*, vol. 54, no. 2, pp. 305–310, Dec. 2008.

[13] P. Azaïs *et al.*, “Causes of supercapacitors ageing in organic electrolyte,” *J. Power Sources*, vol. 171, no. 2, pp. 1046–1053, Sep. 2007.

[14] M. Zhu *et al.*, “Chemical and electrochemical ageing of carbon materials used in supercapacitor electrodes,” *Carbon*, vol. 46, no. 14, pp. 1829–1840, Nov. 2008.

[15] P. Kurzweil and M. Chwistek, “Electrochemical stability of organic electrolytes in supercapacitors: Spectroscopy and gas analysis of decomposition products,” *J. Power Sources*, vol. 176, no. 2, pp. 555–567, Feb. 2008.

[16] R. Nozu, M. Iizuka, M. Nakanishi, and M. Kotani, “Investigation of the life process of the electric double layer capacitor during float charging,” *J. Power Sources*, vol. 186, no. 2, pp. 570–579, Jan. 2009.

[17] H. El Brouji, J.-M. Vinassa, O. Briat, W. Lajnef, N. Bertrand, and E. Woirgard, “Parameters evolution of an ultracapacitor impedance model with ageing during power cycling tests,” in *IEEE Power Electronics Specialists Conference, 2008. PESC 2008*, 2008, pp. 4624–4629.

[18] W. Lajnef, J.-M. Vinassa, O. Briat, H. El Brouji, S. Azzopardi, and E. Woirgard, “Quantification of ageing of ultracapacitors during cycling tests with current profile characteristics of hybrid and electric vehicles applications,” *IET Electr. Power Appl.*, vol. 1, no. 5, pp. 683–689, Sep. 2007.

[19] R. Faranda, “A new parameters identification procedure for simplified double layer capacitor two-branch model,” *Electr. Power Syst. Res.*, vol. 80, no. 4, pp. 363–371, Apr. 2010.

[20] F. Belhachemi, S. Rael, and B. Davat, “A physical based model of power electric double-layer supercapacitors,” in *Conference Record of the 2000 IEEE Industry Applications Conference, 2000*, 2000, vol. 5, pp. 3069–3076 vol.5.

[21] V. Sedlakova *et al.*, “Supercapacitor equivalent electrical circuit model based on charges redistribution by diffusion,” *J. Power Sources*, vol. 286, pp. 58–65, Jul. 2015.

9 AUTHOR'S CURRICULUM VITAE

Dipl. Ing. Tomas Kuparowitz

Education

2013 – *today*	**Brno University of Technology**, Ph.D. degree program, Physical Electronics and Nanotechnology
2011 – 2012	**Brno University of Technology**, Ms.C.. degree program, Cybernetics, Control and Measurements
2008 – 2010	**Brno University of Technology**, Bc. degree program, Automation and Measurement
2005 – 2007	**Gymnázium Brno Vídeňská**, Gymnázium programování 4L

Work experience in the field of study

2014 – *today*	Central European Institute of Technology – Ph.D. student
2008 – 2013	Brno University of Technology, Faculty of Electrical Engineering and Communication, Department of Physics

Short biography

Dipl. Ing Tomas Kuparowitz received his master's degree at Brno University of Technology in the field of Electrotechnics and Communications in 2013. Since then he works on his dissertation thesis on charge transport and storage in supercapacitor structures at the so named University. He absolved internship at EPFL in Lausanne, Switzerland in 2014. From 2014 he was employed by CEITEC BUT at Ph.D. student position, where he works up to present.

Papers in Journals

1. KUPAROWITZ, T.; SEDLÁKOVÁ, V.; SZEWCZYK, A.; HASSE, L.; SMULKO, J.; MAJZNER, J.; SEDLÁK, P.; ŠIKULA, J. Charge Redistribution and Restoring voltage of Supercapacitors. ElectroScope - http://www.electroscope.zcu. cz, 2014, roč. 2014, č. 3, s. 1-7. ISSN: 1802-4564.
2. SEDLÁKOVÁ, V.; ŠIKULA, J.; MAJZNER, J.; SEDLÁK, P.; KUPAROWITZ, T.; BUERGLER, B.; VAŠINA, P. Supercapacitor equivalent electrical circuit model based on charges redistribution by diffusion. Journal of Power Sources, 2015, roč. 2015, č. 286, s. 58-65. ISSN: 0378-7753.
3. KUBERSKÝ, P.; SEDLÁK, P.; HAMÁČEK, A.; NEŠPŮREK, S.; KUPAROWITZ, T.; ŠIKULA, J.; MAJZNER, J.; SEDLÁKOVÁ, V.; GRMELA, L.; SYROVÝ, T. Quantitative fluctuation- enhanced sensing in amperometric NO2 sensors. Chemical Physics, 2015, roč. 456, č. 1, s. 111-117. ISSN: 0301-0104.
4. SZEWCZYK, A.; ŠIKULA, J.; SEDLÁKOVÁ, V.; MAJZNER, J.; SEDLÁK, P.; KUPAROWITZ, T. Voltage dependence of supercapacitor capacitance. METROL MEAS SYST, 2016, roč. 23, č. 3, s. 403-411. ISSN: 0860-8229.

5. SEDLÁKOVÁ, V.; ŠIKULA, J.; MAJZNER, J.; SEDLÁK, P.; KUPAROWITZ, T.; BUERGLER, B.; VAŠINA, P. Supercapacitor degradation assesment by power cycling and calendar life tests. METROL MEAS SYST, 2016, roč. 23, č. 3, s. 345-358. ISSN: 0860-8229.

Papers in Conference Proceedings

6. ŠIKULA, J.; GRMELA, L.; BARTLOVÁ, M.; KUPAROWITZ, T.; KNÁPEK, A.; MÍKA, F. Noise of low-energy electron beam. In 2015 International Conference on Noise and Fluctuations, ICNF 2015. 2015. s. 1-4. ISBN: 9781467383356.
7. SEDLÁKOVÁ, V.; ŠIKULA, J.; SEDLÁK, P.; MAJZNER, J.; KUPAROWITZ, T.; MÍVALT, F.; LANG, M. Supercapacitor Parameters Degradation Analysis by Energy Cycling and Calendar Life Tests. Space Passive Component Days. European Space Agency, 2016. s. 1-13.
8. KUPAROWITZ, T.; SEDLÁKOVÁ, V.; SZEWCZYK, A.; HASSE, L.; SMULKO, J.; MAJZNER, J.; SEDLÁK, P.; ŠIKULA, J. Supercapacitors – Charge Redistribution and Restoring Voltage. In Proceedings. Brno: Vysoké učení technické v Brně, 2014. s. 145-150. ISBN: 978-80-214-4985- 5.
9. KUPAROWITZ, T.; KUPAROWITZ, M. Assessment of Noise Sources in Resistors. In Proceedings of the 21st Student Competition Conference. Brno: Vysoké učení technické v Brně, Fakulta elektrotechniky a komunikačních technologií, 2015. s. 418-422. ISBN: 978-80-214-5148- 3.
10. KUPAROWITZ, M.; KUPAROWITZ, T. Tantalum Capacitor as a MIS Structure: Transport Characteristic Temperature Dependencies. In EEICT proceedings of the 23rd conference. Brno: Vysoké učení technické v Brně, Fakulta elektrotechniky a komunikačních , technologií, 2017. s. 645-649. ISBN: 9788021454965.
11. KUPAROWITZ, T. SUPERCAPACITOR PARAMETERS DEPENDENCE ON CHARGING DURATION. In Proceedings of the 22nd Conference STUDENT EEICT 2016. 1. 2016. s. 680-684. ISBN: 978-80-214-5350-0.
12. KNÁPEK, A.; HORÁČEK, M.; HRUBÝ, F.; ŠIKULA, J.; KUPAROWITZ, T.; SOBOLA, D. Noise behaviour of field emission cathode based on lead pencil graphite. In TECHNICAL DIGEST, 2017 30th International Vacuum Nanoelectronics Conference (IVNC). Herzogssaal Regensburg, Germany: IEEE, 2017. s. 274-275. ISBN: 978-1-5090-3974- 6.
13. KUPAROWITZ, T.; KUPAROWITZ, M. Lead- Acid Battery Evaluation Based on Open Circuit Voltage Fluctuation Measurement. In EEICT proceedings of the 23rd conference. Brno: Vysoké učení technické v Brně, Fakulta elektrotechniky a komunikačních , technologií, 2017. s. 685-689. ISBN: 9788021454965.
14. KUPAROWITZ, T.; SEDLÁKOVÁ, V.; SEDLÁK, P.; ŠIKULA, J. Low frequency noise of electrochemical power sources. In Proceedings of ICNF 2017 Conference, in press
15. KUPAROWITZ, T.; SEDLÁKOVÁ, V.; SEDLÁK, P.; ŠIKULA, J. Supercapacitor Degradation and Reliability. In Proceedings of PCNS 2017 Conference, in press

Research Reports

16. HOLCMAN, V.; JURČÍK, M.; KUPAROWITZ, M.; KUPAROWITZ, T.; PROKOPYEVA, E.; SITA, Z.; ŠKARVADA, P.: Absorb01; Funkční vzorek měření absorpce světla. UFYZ FEKT v Brně. URL: http://www.ufyz.feec.vutbr.cz/veda-a-vyzkum/ produkty.
17. SEDLÁKOVÁ, V.; ŠIKULA, J.; SEDLÁK, P.; MAJZNER, J.; KUPAROWITZ, T. Technical note 11: Modeling of supercapacitors ageing. 2015. s. 1-50.
18. SEDLÁKOVÁ, V.; ŠIKULA, J.; SEDLÁK, P.; MAJZNER, J.; KUPAROWITZ, T.; MÍVALT, F.; LANG, M.; OSTRÝ, L. Equivalent model for AVX MLCC - FINAL REPORT - STAGE II. 2016. s. 1-70.

10 ABSTRACT

Supercapacitor (SC), or electric double-layer capacitor, represents electrical energy device, which offers high power density, short charging time, high number of charging cycles, and long-life duration. This device is of particular interest in fast energy-storage applications.

Detailed study and modeling of the electrical charge transport and its storage is the output of this thesis. Processes, which occur during charging and discharging, are studied and their correlation to fading of SC's parameters is assessed.

New model of SC is proposed. Electric charge stored in SC appears to be divided into two sections. One could be attributed to the Helmholtz capacitance and the other to the diffuse capacitance. The equivalent circuit model contains time dependent resistance $R_D(t)$ between Helmholtz and diffuse capacitances.

While the SC ages, all parameters of equivalent circuit model change. The change of Helmholtz capacitance may be described most accurately by a pure exponential function. Total capacitance follows an exponential stretched law. From experiments it follows, that the greatest influence on SC’s degradation has the amount of transferred energy. The impact of temperature is second most important.

The dependence of equivalent circuit model parameters on ambient temperature before and after aging by discontinuous energy cycling is explored. The value of total capacitance C_T increases linearly with temperature. This is also true for aged samples. The slope for new samples is about 3 times higher than for aged one. The dependence of aging on SC’s equivalent series resistance obeys the quadratic relation. Helmholtz capacitance of SC CapXX 2.75V/2.4F is constant in temperature range 22 °C to 65 °C, with the value of Helmholtz capacitance C_H = 2.78 F for new samples and 2.07 F for aged ones. At temperature range below 22 °C Helmholtz capacitance decreases about 0.5 F due to the aging.

The calendar life tests are devised to simulate SC under light work load at differing ambient temperatures. Temperatures used are from -35 °C up to 65 °C. This experiment is devised to prove that the increased temperature accelerates the electrochemical reactions, which are responsible for SC’s total capacitance degradation.